



2015 International Congress on Ultrasonics, 2015 ICU Metz

Investigation of Scholte and Stoneley Waves in Multi-layered Systems

Onursal Onen* and Yusuf Can Uz

Izmir Institute of Technology, Department of Mechanical Engineering, Izmir Yuksek Teknoloji Enstitusu, Makina Muhendisligi Bolumu Gulbahce Koyu, Urla, Izmir, 35430, Turkey

Abstract

Interface waves are elastic waves that can propagate at the interface between two solids (Stoneley wave) or between a solid and a liquid (Scholte wave). In this study, properties of generalized Stoneley and Scholte waves are investigated analytically in a multi-layer system with both liquid-solid and solid-solid interfaces. The interface waves are modeled using partial waves in layers with finite thicknesses to trace quasi- and non-dispersive modes. Dispersion curves of the propagating modes and corresponding particle displacement profiles are obtained using numerical solution techniques with the global matrix method. Limiting conditions of quasi-modes are evaluated analytically for thickness and material selection. Furthermore, interference of the two interface waves and plate modes are investigated for small frequency-thickness products in the multi-interface system using dispersion curves and particle displacement profiles. Preliminary sensitivity analyses are also performed for development of multi sensing physical quantities such as temperature, viscosity and density simultaneously using interface waves.

© 2015 The Authors. Published by Elsevier B.V. This is an open access article under the CC BY-NC-ND license

(<http://creativecommons.org/licenses/by-nc-nd/4.0/>).

Peer-review under responsibility of the Scientific Committee of ICU 2015

Keywords: Scholte wave, Stoneley wave, interface wave, dispersion, sensor.

1. Introduction

Interface waves are elastic waves that propagate at the interfaces between two media. The interface waves are named as “Stoneley waves” for solid-solid interfaces and “Scholte waves” for solid-liquid interfaces. They are used in sediment characterization, ultrasonics, fluid characterization, and non-destructive testing and evaluation. The energy content of the waves are concentrated in a few wavelengths around the interface in each medium with distribution depending on the material properties of the interfacing media. Scholte wave velocity should be slightly lower than the longitudinal velocity of the fluid and Stoneley wave velocity, should be lower than the smaller of the transverse velocities of the interfacing solids [1]. In this study, properties of Stoneley and Scholte waves are investigated analytically in a multi-layer system generally based on a global-matrix approach [2]. Specifically, with

configurations of i) solid-liquid and solid-solid, ii) liquid-solid-liquid and solid-liquid-solid iii) liquid-solid-solid-liquid, and iv) liquid mixture-solid-liquid mixture with the aim to develop physical multisensory applications. The interface wave sensors are modeled with longitudinal and shear partial waves similarly as Auld [3] and Lowe [2, 4] with solid layers having finite thickness to trace non-dispersive and quasi- modes.

2. Analytical Modeling

The interface waves are modeled following with longitudinal (L) and shear (S) partial waves with their directions (+) or (-) defined with respect to positive x_2 direction as seen in figure 1. At the semi-infinite half spaces of liquids, only the waves directed away from the interface, and in the intermediate layers all four partial waves are considered. Following the convention of Lowe, continuity of the displacements in x_1 and x_2 , and continuity of the stresses in 11 and 12 directions at the interfaces are considered. Readers may refer to Lowe [2] for derivations and expressions of the displacements and stresses. Instead of matrices for top and bottom of the layer, column vectors for each partial wave is used and the global matrix for any scenario can be formed using proper arrangement of these column vectors. For example, the four layer system seen in the figure 1 can be defined as in the matrix in equation 1 below. The wave vector W and the four partial wave column vectors is given in equation 2, where $\alpha = \sqrt{(\lambda + 2\mu) / \rho}$, $\beta = \sqrt{\mu / \rho}$, $C_\alpha = \sqrt{\omega^2 / \alpha^2 - k^2}$, $C_\beta = \sqrt{\omega^2 / \beta^2 - k^2}$, $g_\alpha = \exp(iC_\alpha x_2)$, $g_\beta = \exp(iC_\beta x_2)$; ρ is density λ and μ are the Lamé constants, ω is the angular speed, α is the bulk longitudinal and β is the bulk shear velocity and k is the wavenumber. The “A” values correspond to amplitudes of the each represented partial wave. Regions highlighted in blue dash lines corresponds to the quasi-Scholte modes and in red dash lines correspond to the problems of non-dispersive interface waves (Stoneley in the center and Scholte at the corners).

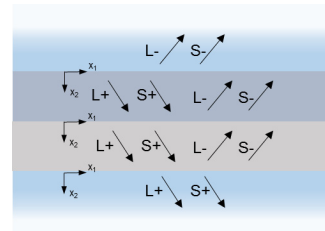


Figure 1. General overview of system

$$\begin{bmatrix} -(L_{1,-}) & -(S_{1,-}) & (L_{2,+}) & (S_{2,+}) & (L_{2,-}) & (S_{2,-}) & 0 & 0 & 0 & 0 & 0 & 0 \\ 0 & 0 & (L_{2,+}) & (S_{2,+}) & (L_{2,-}) & (S_{2,-}) & -(L_{3,+}) & -(S_{3,+}) & -(L_{3,-}) & -(S_{3,-}) & 0 & 0 \\ 0 & 0 & 0 & 0 & 0 & 0 & -(L_{3,+}) & -(S_{3,+}) & -(L_{3,-}) & -(S_{3,-}) & (L_{4,+}) & (S_{4,+}) \end{bmatrix} \quad (1)$$

$$\begin{bmatrix} A_{(L_{1,-})} & A_{(S_{1,-})} & A_{(L_{2,+})} & A_{(S_{2,+})} & A_{(L_{2,-})} & A_{(S_{2,-})} & A_{(L_{3,+})} & A_{(S_{3,+})} & A_{(L_{3,-})} & A_{(S_{3,-})} & A_{(L_{4,+})} & A_{(S_{4,+})} \end{bmatrix}^T = 0$$

$$W = \begin{pmatrix} u_1 \\ u_2 \\ \sigma_{22} \\ \sigma_{12} \end{pmatrix}, L_+ = \begin{pmatrix} kg_\alpha \\ C_\alpha g_\alpha \\ iB\rho g_\alpha \\ i2\beta^2 k C_\alpha \rho B g_\alpha \end{pmatrix}, S_+ = \begin{pmatrix} C_\beta g_\beta \\ -kg_\beta \\ -i2\beta^2 k C_\beta \rho B g_\beta \\ i\rho B g_\beta \end{pmatrix}, L_- = \begin{pmatrix} k / g_\alpha \\ -C_\alpha / g_\alpha \\ iB\rho / g_\alpha \\ -i2\beta^2 k C_\alpha \rho B / g_\alpha \end{pmatrix}, S_- = \begin{pmatrix} -C_\beta / g_\beta \\ -k / g_\beta \\ i2\beta^2 k C_\beta \rho B / g_\beta \\ i\rho B / g_\beta \end{pmatrix} \quad (2)$$

The solution of the system for the phase velocity can be done by numerically solving for the phase velocities which make the determinant zero. The results of the model and numerical calculations was verified with the free demo version of DISPERSE software with titanium and motor oil for pure and quasi-Scholte modes and also with multiple results from literature.

3. Results

Dispersion curves and corresponding displacement profiles are obtained for several configurations and materials. For solids, aluminum, steel, Pyrex glass, and a hypothetical plastic-like material (obtained with varying the values of bulk velocities and density for high sensitivity) are chosen and water, motor oil, ethanol, glycerol; and mixtures of water-glycerol and water-ethanol are selected for liquids. The material properties used are listed in table 1, obtained from [1]. The dispersion curves of only the interface waves are included in all figures.

3.1. Interface of two semi-infinite layers

Firstly, dispersion curves and displacement profiles are obtained and investigated for non-dispersive Scholte and Stoneley waves with single interface at the boundary of two semi-infinite media. Solid materials: glass, steel, and aluminum and liquids: water, oil, glycerol, and motor oil are investigated in a matrix of solid-solid and solid liquid couples with dispersion curves. This was essential to trace the complex three and four layer system interface waves, whose interface velocities should asymptotically approach pure interface wave velocities. Note that, glass and steel were selected as they support Stoneley waves. The results of the non-dispersive interface wave velocities and the displacement profiles are obtained to be used in tracing the quasi-interface waves in multi-layered system.

Table 1. Material Properties

| Material | Density (kg/m ³) | V _l (m/s) | V _s (m/s) |
|----------|------------------------------|----------------------|----------------------|
| Steel | 7700 | 5939 | 3283 |
| Aluminum | 2700 | 5919 | 2981 |
| Glass | 2300 | 5637 | 3297 |
| Water | 1000 | 1480 | - |
| Glycerol | 1261 | 1930 | - |
| Ethanol | 789 | 1144 | - |

3.2. Interfaces of a finite-thickness layer enclosed by two semi-infinite layers

Following the pure non-dispersive modes, interface waves has been investigated with a solid layer between two identical semi-infinite spaces, a fluid layer between two identical solid semi-infinite layers and additional configurations of solids and fluids. Dispersion curves are presented for different configurations with 1 mm middle layer thickness for water-aluminium/steel/glass-water, ethanol/glycerine-steel-ethanol/glycerine, aluminium-water-glass, and steel-glass-steel and glass-steel-glass configurations.

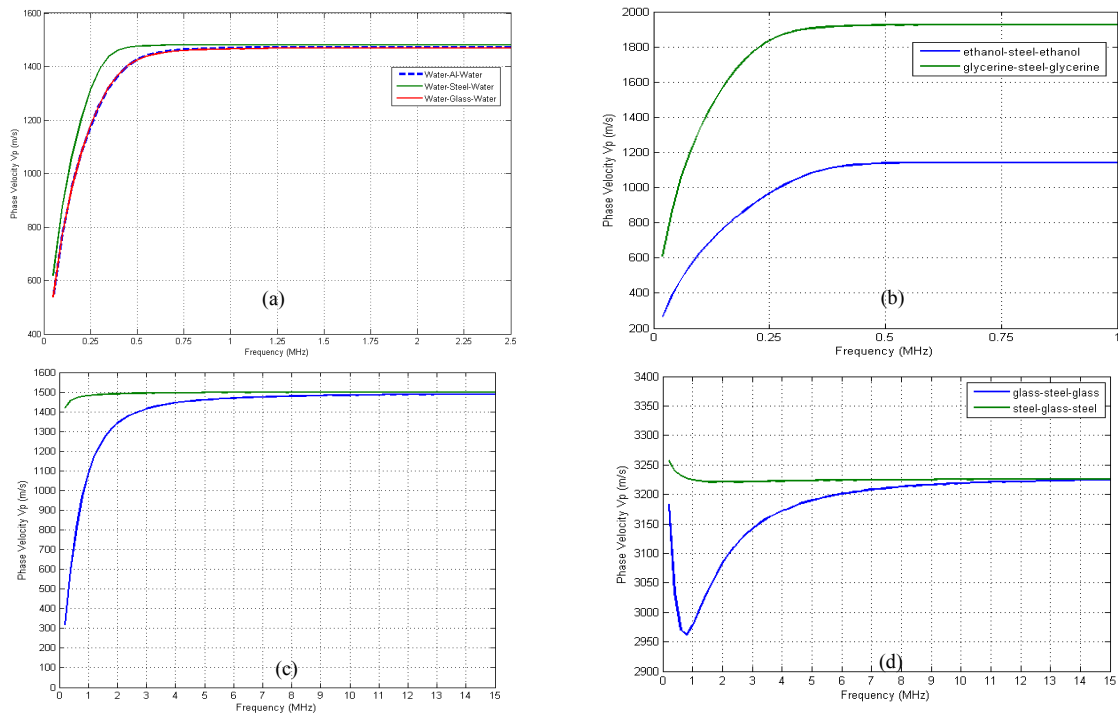


Figure 2. Dispersion curves for different configuration with 1 mm middle layer thickness: a) water-aluminium/steel/glass-water, b) ethanol/glycerine-steel-ethanol/glycerine, c) aluminium-water-glass d) steel-glass-steel and glass-steel-glass

3.3. Interfaces of two finite-thickness layers enclosed by two semi-infinite layers

The four layer system is then investigated, with two finite thickness layers enclosed by two semi-infinite fluid layers in different configurations, and results of these are presented in figures 3 and b. Two thin layers of glass, steel and the hypothetical plastic-like material with properties $\rho=1200\text{kg/m}^3$, $V_1=3200\text{ m/s}$ and $V_s=1650\text{ m/s}$. The material has been optimized manually to show the greatest sensitivity to changing concentrations. The density and longitudinal velocities used are listed in table 2.

Table 2. Properties of ethanol-water mixture [5].

| % Ethanol Conc. | 10 | 20 | 30 | 40 | 50 | 60 | 70 | 80 | 90 |
|-----------------------------|------|------|------|------|------|------|------|------|------|
| V_1 (m/s) | 1544 | 1606 | 1612 | 1575 | 1518 | 1454 | 1394 | 1337 | 1284 |
| Density (kg/m^3) | 982 | 969 | 954 | 935 | 913 | 891 | 868 | 843 | 818 |

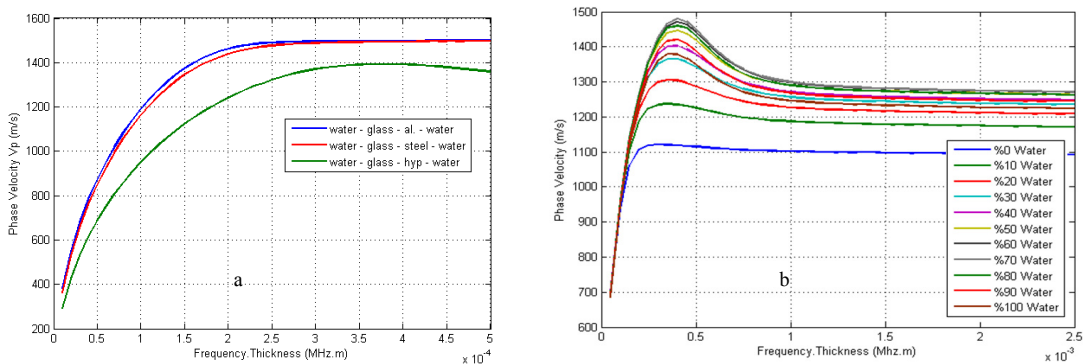


Figure 3. Dispersion curves for four layer configuration with varying middle layer thickness frequency products: a) water-glass-aluminium/steel/hypothetical material-water, b) hypothetical material in the extended range with $\rho=1200\text{kg/m}^3$, $V_1=3200\text{ m/s}$ and $V_s=1650\text{ m/s}$ for varying concentrations of ethanol-water mixture..

3.4 Sensitivity of Scholte waves to ethanol- and glycerol-water mixtures with different concentrations.

The last problem investigated is for use of Scholte waves to quantify the concentrations of these mixtures, using ultrasonic interface waves. The change in Scholte velocities are calculated using dispersion curves and non-dimensional Scholte wave graph, which are presented in the figures 4 a and b for steel and plastic material as the mid layer with 1 mm thickness. All the results for three layer and four layer cases are summarized in figure 5.

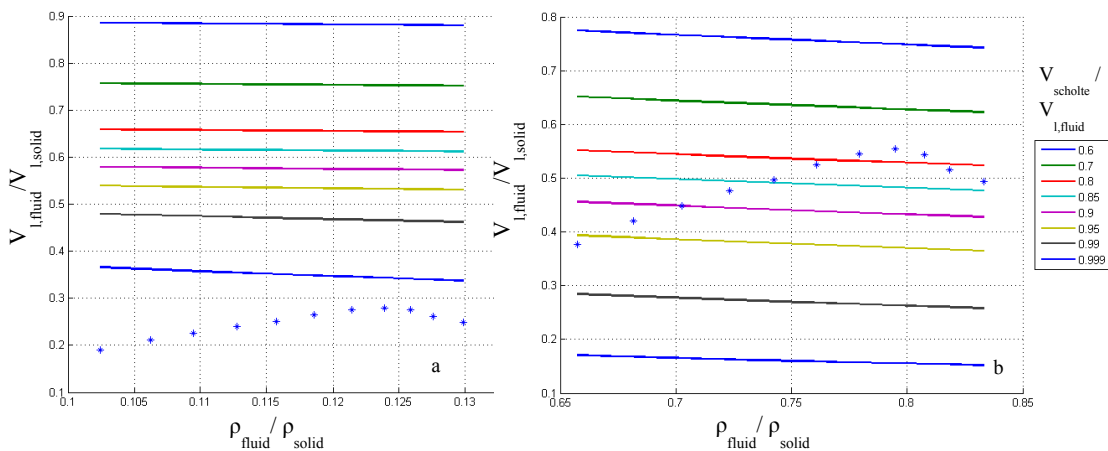


Figure 4. Scholte wave velocities of water-ethanol mixtures with varying concentrations. Poisson’s ratio: 0.28, x-axis: $\rho_{\text{fluid}}/\rho_{\text{solid}}$, Y-axis: $V_{1,\text{fluid}}/V_{1,\text{solid}}$, contours: $V_{\text{scholte}}/V_{1,\text{fluid}}$, stars: $V_{\text{scholte}}/V_{1,\text{fluid}}$ values for increasing concentrations. a) steel, b) plastic.

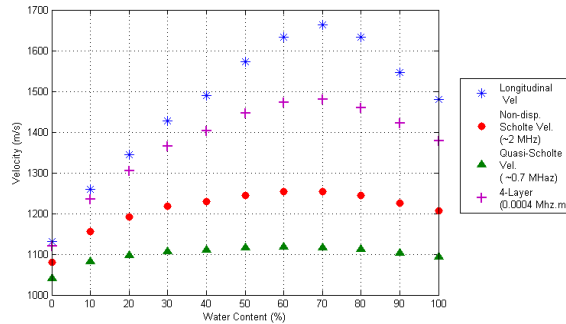


Figure 5. Overview of longitudinal velocity, non-dispersive Scholte wave velocity for mixture-plastic-mixture, quasi-Scholte wave velocity for three layer with $f=0.7$ MHz for mixture-plastic-mixture and quasi-Scholte wave velocity for mixture-glass-plastic-mixture for 0.0004 MHz.mm.

4. Conclusions

In this study dispersion curves for three layer and four layer systems to trace quasi and non-dispersive Scholte modes are presented in order to develop fluid property sensors. For the three layer case, as presented in 3.2, the transition from quasi- to non-dispersive modes are sharper for solids with high speed of sound velocities and densities, and when speed of sound in liquid is closer to shear velocity of the solid. For a fluid enclosed by different solids, Scholte waves of both interfaces present, with sharper change in the Scholte wave stiffer solid and fluid. Finally, for the Stoneley wave, two different regimes are observed, depending on stiffer material being at the middle or at the half spaces. For both cases, the material in the half space dominates the Stoneley wave at the lower frequencies. For the four layer case, what determines the limiting interface wave velocity is the smaller of the shear velocity of the solids and liquid longitudinal velocity. A more dramatic change is observed when a plastic like hypothetical material is tested, with Scholte speed firstly approaching to shear velocity of stiffer solid and then to less stiff solid. Finally, for the case in which the sensitivity of Scholte waves to changing concentrations of water-ethanol mixture. As seen in Figure 4-a, a typical waveguide material like steel show no sensitivity, however with the same plastic material the sensitivity dramatically increases, which means with proper material selection, i.e. density and shear velocity of solid being slightly higher than density and speed of sound in the fluid, dramatic change in Scholte wave velocity with changing concentrations can be observed with proper configurations. Zero phase velocity regions are observed for many configurations that can be of interest for sensing applications.

Acknowledgement

This work is supported by The Scientific and Technological Research Council of Turkey (TÜBİTAK) through grant 114C102.

References

1. Meegan, G.D., et al., *Nonlinear Stoneley and Scholte waves*. The Journal of the Acoustical Society of America, 1999. **106**(4): p. 1712-1723.
2. Lowe, M.J.S., *Matrix Techniques for Modeling Ultrasonic-Waves in Multilayered Media*. Ieee Transactions on Ultrasonics Ferroelectrics and Frequency Control, 1995. **42**(4): p. 525-542.
3. Auld, B.A., *Acoustic fields and waves in solids*. 2nd ed. 1990, Malabar, Fla.: R.E. Krieger.
4. Cegla, F.B., *Ultrasonic Waveguide Sensors for Fluid Characterisation and Remote Sensing*, in *Department of Mechanical Engineering*. 2006, Imperial College London: London, UK. p. 248.
5. B. Liu and A.B. Koc, *Ultrasonic determination of water concentration in ethanol fuel using artificial neural networks*. Transactions of the American Society of Agricultural and Biological Engineers, 2012. **55**(5): p. 1865-1872.